Available online at www.sciencedirect.com
SCIENCE DIRECT®
Journal of Theoretical Biology 234 (2005) 49–65
Journal of Theoretical Biology
www.elsevier.com/locate/yjtbi

A dynamic model of mouth closing movements in clariid catfishes: the role of enlarged jaw adductors

Sam Van Wassenbergh[a,*], Peter Aerts[a], Dominique Adriaens[b], Anthony Herrel[a]

[a]*Department of Biology, University of Antwerp (U.A.), Universiteitsplein 1, B-2610 Antwerpen, Belgium*
[b]*Vertebrate Morphology, Ghent University (UGent), K.L. Ledeganckstraat 35, B-9000 Gent, Belgium*

Received 20 July 2004; received in revised form 3 November 2004; accepted 4 November 2004
Available online 13 December 2004

Abstract

Some species of Clariidae (air breathing catfishes) have extremely large (hypertrophied) jaw closure muscles. Besides producing higher bite forces, the enlarged muscles may also cause higher accelerations of the lower jaw during rapid mouth closure. Thus, jaw adductor hypertrophy could potentially also enable faster mouth closure. In this study, a forward dynamic model of jaw closing is developed to evaluate the importance of jaw adductor hypertrophy on the speed of mouth closure. The model includes inertia, pressure, tissue resistance and hydrodynamic drag forces on the lower jaw, which is modelled as a rotating half-ellipse. Simulations are run for four clariid species showing a gradual increase in jaw adductor hypertrophy (*Clarias gariepinus*, *Clariallabes longicauda*, *Gymnallabes typus* and *Channallabes apus*). The model was validated using data from high-speed videos of prey captures in these species. In general, the kinematic profiles of the fastest mouth closure from each species are reasonably well predicted by the model. The model was also used to compare the four species during standardized mouth closures (same initial gape angle, travel distance and cranial size). These simulations suggest that the species with enlarged jaw adductors have an increased speed of jaw closure (in comparison with the non-hypertrophied *C. gariepinus*) for short lower jaw rotations and when feeding at high gape angles. Consequently, the jaw system in these species seems well equipped to capture relatively large, evasive prey. For prey captures during which the lower jaw rotates freely over a larger distance before impacting the prey, the higher kinematic efficiency of the *C. gariepinus* jaw system results in the fastest jaw closures. In all cases, the model predicts that an increase in the physiological cross-sectional area of the jaw muscles does indeed contribute to the speed of jaw closure in clariid fish.
© 2004 Elsevier Ltd. All rights reserved.

Keywords: Forward dynamics; Feeding; Prey capture; Jaw movements; Muscle hypertrophy

1. Introduction

By closing the mouth rapidly, predators may reduce the chance of prey escape. Especially when feeding on quickly moving, elusive prey, a fast snapping of the oral jaws onto the prey can be an important aspect of the predator's prey capture success (Wainwright and Richard, 1995). In fishes, such fast mouth closings also contribute to overall suction feeding performance as it excludes the reversal of flow of water (and prey) sucked into the buccal cavity (Muller and Osse, 1984; Muller et al., 1982). Hence, several experimental studies on prey capture kinematics of adult fishes have reported extremely rapid mouth closures occurring even within 20 ms (Aerts, 1990; Gibb, 1995; Lauder, 1980; Lauder and Norton, 1980).

In Actinopterygian fishes, the *musculus adductor mandibulae* complex powers these jaw closing movements. According to Newton's second law of motion, increased forces generated by this muscle complex

*Corresponding author. Tel.: +32 3820 2260; fax: +32 3820 2271.
E-mail addresses: Sam.VanWassenbergh@ua.ac.be (S. Van Wassenbergh), Peter.Aerts@ua.ac.be (P. Aerts), dominique.adriaens@UGent.be (D. Adriaens), anthony.herrel@ua.ac.be (A. Herrel).

0022-5193/$ - see front matter © 2004 Elsevier Ltd. All rights reserved.
doi:10.1016/j.jtbi.2004.11.007

during lower jaw adduction will cause higher accelerations. Consequently, a given jaw closing velocity can be reached in less time. The importance of an increased force from the jaw muscles to the speed of mouth closing has also been illustrated experimentally in unloading experiments in humans (Nagashima et al., 1997; Slager et al., 1997, 1998; Van Willigen et al., 1997). In these studies, during which resistance to a forceful isometric bite is suddenly withdrawn, significantly higher mouth closing velocities are reached when prior to mouth closure (and consequently also during mouth closure) higher bite forces are exerted.

Some species of Clariidae (air breathing catfishes) have extremely well developed (hypertrophied) adductor mandibulae muscles (Cabuy et al., 1999; Devaere et al., 2001; Herrel et al., 2002) (Fig. 1). The biological role of this jaw adductor hypertrophy, which is assumed to be a derived feature that originated several times independently in clariids (Teugels and Adriaens, 2003), is still unclear. Diet analyses (Huysentruyt et al., 2004) found a remarkably large proportion of hard prey types in the species with the most extreme jaw adductor hypertrophy. On the other hand, most species also include small, agile prey such as fishes into their diet. Furthermore, a kinematic study of prey capture in a clariid species with a moderate degree of jaw adductor hypertrophy (*Clariallabes longicauda*; Fig. 1) has demonstrated that even non-evasive prey types (which could be caught with minimal movement of the oral jaws) are caught using considerable expansions of the cranial system followed by a fast snapping the jaws on the prey (Van Wassenbergh et al., 2004).

Biomechanical modelling has demonstrated that the enlarged jaw muscles in clariid catfishes drastically increase the maximal biting force of these species under fully static conditions (i.e. without any movement involved; Herrel et al., 2002). As increased forces from the jaw muscles can also result in larger moments of force that drive the lower jaw rotation during jaw closure, higher accelerations can be expected as well. Thus, besides enhancing the performance during static jaw closure (e.g., crushing hard prey or tearing pieces from large prey) the enlargement of the jaw adductor muscles could also be used to power fast snapping of the jaws.

The main objective of the present study is to test whether the observed increase in the dimensions of the jaw adductor muscles in clariid catfishes could be used to develop increased velocities of mouth closure. To test this idea, a forward dynamic model of jaw closing is developed and validated using experimental data from prey capture in clariid catfishes. By comparing simulated jaw closing events from clariid species with jaw closer dimensions ranging from relatively slender (*Clarias gariepinus*) to extremely large (*Channallabes apus*) (Fig. 1) under standardized conditions (same initial gape angle, travel distance and absolute cranial size), the role of the jaw adductor enlargement in generating higher mouth closing velocities is evaluated. Additionally, the effects of changes in several aspects of the oral jaw apparatus (e.g. cross-sectional area, pennation angle, fibre length, orientation of the jaw adductors,

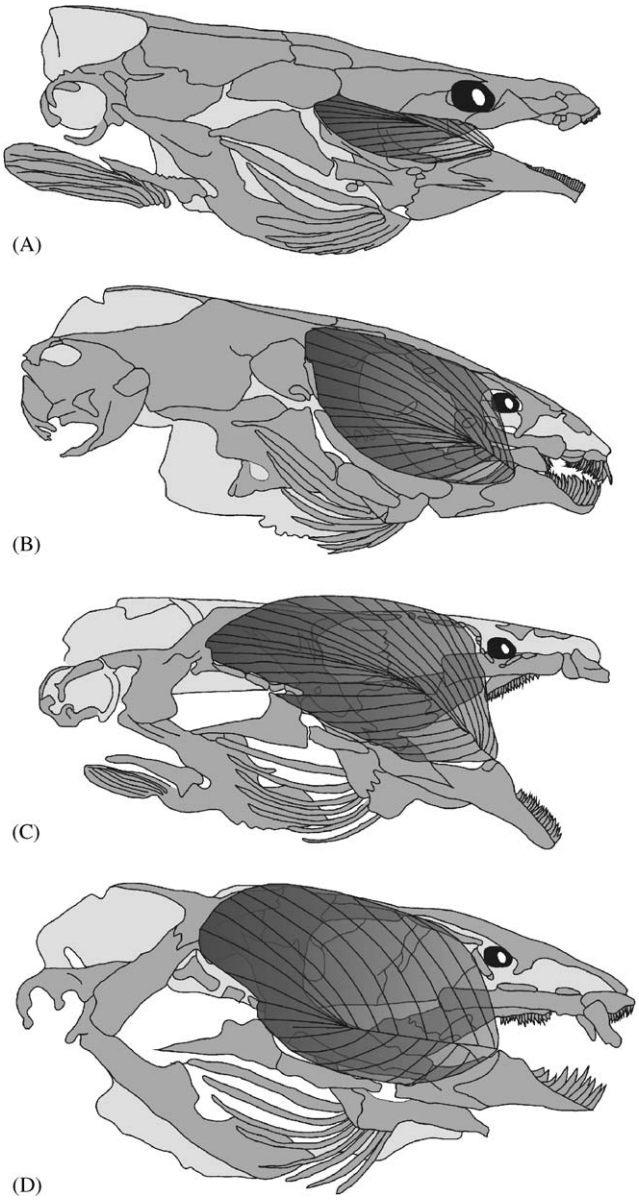

Fig. 1. Lateral view on the osteocranium and the jaw adductor muscles (in dark grey) of four clariid species with increasing size of the jaw adductors (from A to D). A = *Clarias gariepinus*, B = *Clariallabes longicauda*, C = *Gymnallabes typus* and D = *Channallabes apus*. A and C are modified after Cabuy et al. (1999), B after a study by L. Van Meir (personal communication) and D after Devaere et al. (2001). In *C. gariepinus*, a part of the muscle complex is covered by bones. A modelling study by Herrel et al. (2002) showed that, for example, maximal static bite force at the anteriormost teeth (oriented perpendicular to the lower jaw) of specimens with cranial lengths of 39 mm is much higher in *G. typus* (6.88 N) and *C. apus* (13.81 N) than for *C. gariepinus* (1.2 N).

dimensions of the lower jaw, length and inclination of the lower jaw in-lever) on the speed of mouth closure can be assessed using this model.

2. Materials and methods

2.1. The model

The lower jaw adduction is modelled as a rotation of a half-elliptic surface (Fig. 2). Detailed morphological analyses (Adriaens and Verraes, 1997; Cabuy et al., 1999, Devaere et al., 2001) have shown that the lower jaw of clariid catfishes closely resembles the shape of a half-ellipse. Also in other teleost fishes, for example Cichlidae, this resemblance has been noticed and has subsequently been used in modelling studies (Aerts et al., 1987). As the space between left and right lower jaws is largely taken up by skin and muscles (*m. protractor hyoideus*, *m. intermandibularis, m. hyohyoideus inferior*), a half-elliptic surface is chosen over a half-elliptic bar as a model for the rotating lower jaw.

Upward rotation of the lower jaw is caused by the contraction of the jaw adductor muscles. We modelled the instantaneous force output of these muscles during mouth closure, taking into account the physiological characteristics of contracting muscle (activation rise time, force–velocity relationship, force–length relationship, passive parallel elastic forces). By modelling the lower jaw and its inertial properties together with forces that cause (jaw muscle force) and resist (drag, pressure differences, tissue resistance) jaw closing movements, adduction of the lower jaw can be simulated. Simulations were run with a time step of 0.01 ms. Until the next simulated point, the acceleration was kept constant. To avoid circularities in the formulae, the acceleration at time t is calculated based on the velocity and gape angle at $t = -0.01$ ms. At the start of the simulation (-0.01 ms before the start of jaw closing, i.e. time 0), an acceleration of 0 rad/s^2 was imposed.

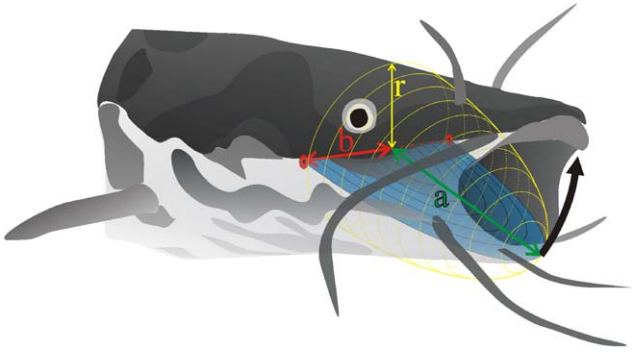

Fig. 2. Representation of the half-elliptic surface (in blue) as a model of the lower jaw in *C. gariepinus*, with *a* the length (in green) and *b* the half width of the ellipse at the axis of rotation (in red). The half-ellipsoid added mass component with radius *r* is shown in yellow.

2.1.1. Equation of motion

In a dynamic equilibrium situation, the equation of angular motion for the rotating jaw is determined by the sum of all moments of force acting on the system. The following equation of motion was used:

$$I\ddot{\alpha} = M_m + M_d + M_{pr}, \quad (1)$$

where I is the moment of inertia of the lower jaw with respect to the quadratomandibular axis of rotation, $\ddot{\alpha}$ the angular acceleration of the lower jaw, M_m, M_d and M_{pr} are the moments of force from, respectively, the jaw muscles, hydrodynamic drag and pressure differences between inside and outside the buccal cavity, together with tissue resistance. As the density of the lower jaw and its surrounding soft tissues is approximately the same as the density of the water, gravitational forces and hydrostatic lift are assumed to counter each other, and are not considered further.

2.1.2. Inertia of the lower jaw

When an object moves through water, it will put in motion a significant amount of water as well (Daniel, 1984). Therefore, an added mass component was included in the model (Fig. 2). As added mass, a volume of water with the shape of a half-ellipsoid comprising the half-ellipse was taken. This was done in accordance with studies on fish swimming hydrodynamics (Vogel, 1994). At each point along the length axis of the lower jaw, the radius of this half-ellipsoid equals the half width of the half-ellipse. The moment of inertia (I) of a half-elliptic surface and its half-ellipsoid added mass rotating around the minor axis (b in Fig. 2) can be calculated after expressing the mass distribution as a function of the distance from the axis of rotation. We simplified the calculations by assuming that the mass of each cylindrical segment of the ellipsoid at a given distance from the axis of rotation, is centred in the middle:

$$I = (2/15)\pi\rho a^3 b^2, \quad (2)$$

where ρ is the density of water (1000 kg/m^3), a the length of the lower jaw and b the half width of the lower jaw. The assumption was made that the added mass component remained constant during the entire mouth closing phase.

2.1.3. Drag

We accounted for drag forces on the lower jaw surface that were generated by the rotation of the lower jaw itself, as if it were moving in motionless water. Drag forces (F_d) are given by the following formula:

$$F_d = -(1/2)C_d A\rho v^2, \quad (3)$$

where C_d is the shape-dependent drag coefficient, A the area of the half-ellipse, ρ the density of the fluid ($1000\,kg/m^3$) and v the linear velocity of fluid flow. The drag coefficient of 2 from Lasher (2001) was used (flow normal to a flat plate). During rotation, the linear velocity of a given point on the half elliptic surface depends on its distance to the axis of rotation. Therefore, when calculating the moment of force from drag, the area of the half-ellipse was expressed as a function of its distance from the axis of rotation (x):

$$M_d = -\int_0^a (b/a)\sqrt{a^2 - x^2}(\omega x)^2 \rho x \, dx, \quad (4)$$

with a the length and b the half width of the half-ellipse, ω the angular velocity of rotation and ρ the water density. Under these conditions, the moment of force from drag forces on a rotating half elliptic surface is given by

$$M_d = -(2/15)\rho\omega^2 a^4 b. \quad (5)$$

2.1.4. Buccal pressure and tissue resistance

The buccal cavity will decrease in volume during jaw closure. This usually results in a positive pressure inside the buccal cavity (Van Leeuwen and Muller, 1983). Although the magnitudes of these pressures are typically much lower than the negative pressures during the expansive phase (generating suction), they could still have an important effect on the movements of the lower jaw. Besides this positive intra-oral pressure, movements of the jaws are also dampened by the surrounding soft tissues (Koolstra and Van Eijden, 1996). Unfortunately, estimates of pressures inside the buccal cavity during prey capture of catfish, as well as data on the effect of tissue resistance on jaw movements are lacking. Therefore, a factor is added into the model that includes both forces from positive buccal pressures and soft tissue resistance. Both pressure and tissue resistance are likely to increase when the lower jaw is lifted towards the roof of the buccal cavity as the buccal cavity is increasingly reduced in volume and tissues connecting the hyoid apparatus to the lower jaw (*musculus protractor hyoideus*) are stretched.

In Van Leeuwen and Muller (1983), estimates of buccal pressure at specific positions along the sagittal axis of the head are presented for a variety of fish species. As positive pressure peaks at the end of prey capture strongly depend on the approaching speed of the predatory fish, the peak pressure of +1 kPa halfway the buccal cavity in the slowest fish (*Onchorynchus mykiss*; Van Leeuwen and Muller, 1983) is likely the best assessment of buccal pressure during jaw closure in a catfish, which also approach the prey relatively slowly (Van Wassenbergh et al., 2004). We (arbitrarily) assumed that dampening as a result of tissue resistance would be of the same order of magnitude. This factor also includes some resistance to lower jaw rotation as a result of friction at the jaw joint. Thus, the following formula was used to account for intra-oral pressure and soft tissue resistance:

$$M_{pr} = -0.40373(\pi/2)a^2 bP, \quad (6)$$

where ($0.40373^* a$) is the distance from the rotation axis of the center of area of the half-ellipse, ($a^* b^* \pi/2$) the total area of the half-ellipse. In this formula, pressure P is a function that starts at 0 Pa (beginning of mouth closure), increases linearly with decreasing gape angle, and reaches the peak value of +2 kPa at the end of mouth closure. This pressure profile is assumed to be uniform over the half-elliptic surface representing the lower jaw.

2.1.5. Oral jaw apparatus

The lever system of the lower jaw and the jaw muscles is schematically represented in Fig. 3. As the upper jaw of catfishes is fixed to the neurocranium, no protrusion of the jaws occurs in this group of fishes (Alexander, 1965). Consequently, the mouth is opened and closed by a simply rotation the lower jaw around the quadrato-mandibular joint. The adductor mandibulae muscle complex of clariid catfishes consists of two parts: an external A2A3′ part and a smaller, medial A3″ part (Adriaens and Verraes, 1996). Whereas the A2A3′ part is a bipennate muscle, the A3″ is not. For fast jaw closure, a bilateral symmetrical activity of these jaw muscles can be assumed. As in that case, left and right transversal force components are expected to cancel each other out, only the sagittal orientation of both jaw

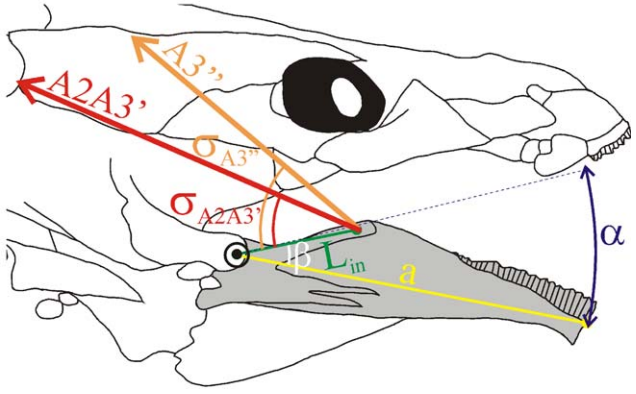

Fig. 3. Schematic representation of the lower jaw lever system in Clariidae in lateral view. The *musculus adductor mandibulae* A2A3′ and A3″ are represented by their lines of action (red and orange, respectively). Both muscles insert on the coronoid process of the lower jaw (in grey). The distance from the jaw muscle attachment to the centre of rotation of the lower jaw (L_{in}, lower jaw in-lever, green line) and the lower jaw length axis (a, yellow line) are shown. β is the angle between the in-lever (L_{in}) and out-lever (a) (also referred to as the inclination of the lower jaw in-lever). $\sigma_{A2A3'}$ and $\sigma_{A3''}$ are the angles between L_{in} and the lines of action of, respectively, A2A3′ and A3″ (also referred to as the inclination of the jaw muscles with regard to the in-lever).

muscle parts (A2A3′ and A3″) was taken into account. As the origin of the jaw muscles is fixed to the neurocranium, the orientation of the lines of action of these muscles is solely determined by the degree of lower jaw depression. Biometric data on all variables represented in Fig. 3 were taken from the literature (Cabuy et al., 1999; Devaere et al., 2001; Herrel et al., 2002) for all four species (Fig. 1; Table 1). All linear biometric variables were scaled to cranial length (defined as the distance between the rostral tip of the premaxilla and the caudal tip of the occipital process), assuming isometric scaling of the morphological variables in Table 1.

2.1.6. Muscular torque

At each point in time, the moment exerted by the jaw muscles (M_m) is a function of gape angle and the force generated by the jaw muscles ($F_{A2A3'}$ and $F_{A3''}$):

$$M_m = F_{A2A3'} \sin(\sigma_{A2A3'})L_{in} + F_{A3} \sin(\sigma_{A3''})L_{in}, \quad (7)$$

where σ will decrease with increasing gape angle (Fig. 3). The instantaneous muscle force depends on several dynamical muscle properties. In our model, we accounted for the force–velocity dependence (F_{FV} factor), force–length dependence (F_{FL} factor), parallel elastic forces (F_{Par} factor) and a "rise time" of activation of the muscle (F_{Act} factor):

$$F_{Muscle} = F_{Max} * F_{FV} * F_{FL} * F_{Act} + F_{Par}, \quad (8)$$

where F_{Max} (maximal force along the line of action of the muscle) is given by the following formula:

$$F_{Max} = PCSA * F_{Max\,Fibre} * \cos(\theta), \quad (9)$$

with $PCSA$ the physiological cross-section area of the muscle (volume divided by average fibre length), $F_{Max\,Fibre}$ the maximal isometric force that can be generated by the muscle fibres and θ the average pennation angle of the muscle fibres. The value of $19\,N/cm^2$ (Akster et al., 1985) was used for $F_{Max\,Fibre}$, as this is the highest value from experimental measurements of contractile properties of fast fibred fish head muscles out of several studies (Akster et al., 1985; Flitney and Johnston, 1979; Granzier et al., 1983; Johnston, 1982, 1983).

When a pennate muscle is stretched, the pennation angle of muscle will decrease and subsequently the component of force parallel to the line of action of the muscle will increase (see Eq. (9)). Therefore, during lower jaw movements, F_{Max} depends on the degree of lower jaw depression. For calculating the relation between length of the muscle (origin to insertion) and average pennation angle, we followed Narici (1999):

$$\theta_2 = \tan^{-1}\left(\frac{FL_1\, sin(\theta_1)}{FL_2\, \cos(\theta_1) + (L_2 - L_1)}\right), \quad (10)$$

with FL = average fibre length, θ = average pennation angle and L = origin to insertion muscle length, at two muscle elongation positions (subscript 1 and 2). As FL, θ and L in a closed mouth situation is known for the four clariids from Herrel et al. (2002), these variables can be calculated for each muscle length by the above formula. Next, the instantaneous fibre length can be calculated using the following equation:

$$FL_2 = FL_1 \sin(\theta_1)/\sin(\theta_2). \quad (11)$$

2.1.7. Force–velocity factor

Once a muscle fibre starts shortening, the maximal force that can be generated by this fibre will decrease. The relationship between contraction velocity of muscle fibres and their force output is characterized by the following Hill's equation:

$$F_{FV} = (V_{Max} - v)/(V_{Max} + Gv), \quad (12)$$

where F_{FV} is the force–velocity factor, V_{Max} the maximal unloaded contraction velocity, v the fibre shortening velocity at a given time and G a constant

Table 1
Biometric data of lower jaw lever system

Species	a	b	L_{in}	β		$\sigma(\alpha = 0°)$	Muscle length ($\alpha = 0°$)	$PCSA$	Avg. pen angle	Avg. fibre length
Clarias gariepinus	0.2869	0.2145	0.0750	23.66	A2A3′	39.35	0.2588	0.01194	27.35	0.115
					A3″	57.40	0.2086	0.00626		0.125
Clariallabes longicauda	0.3027	0.2624	0.1197	31.26	A2A3′	51.35*	0.3887*	0.02563*	44.37*	0.104*
					A3″	59.08*	0.2910*	0.00776*		0.098*
Gymnallabes typus	0.3797	0.2686	0.1373	24.97	A2A3′	49.30	0.4304	0.03907	50.72	0.113
					A3″	63.47	0.2710	0.00702		0.093
Channallabes apus	0.3609	0.2558	0.1456	43.64	A2A3′	61.27	0.4086	0.08351	35.14	0.135
					A3″	76.93	0.2877	0.01124		0.117

a = lower jaw length, b = half width lower jaw, L_{in} = length of lower jaw in-lever, σ = angle between L_{in} and the jaw muscle line of action, α = mouth opening angle (see also Fig. 3), PCSA = physiological cross sectional area (both sides included), Avg. pen angle = average pennation angle. All length values are in numbers of cranial lengths. All angle variables are in degrees. The given muscle lengths are distances of origin to insertion in the sagittal plane. *data for *Clariallabes melas*. Data on muscle dimensions and orientations are from Herrel et al. (2002). Other data are obtained from Adriaens and Verraes (1996) (*C. gariepinus*), Liesbeth Van Meir (personal communication) (*C. longicauda*), Cabuy et al. (1999) (*G. typus*) and Devaere et al. (2001) (*C. apus*). Note that the A3″ muscle is not pennate.

determining the shape of the Hill-curve, with G roughly being equal to 4 in vertebrate muscle (Hill, 1970; Alexander, 2003). The value of 8.4 muscle lengths per second from Johnston and Brill (1984) was used for V_{Max}, as this is the highest value for fast-fibred fish muscles out of numerous studies (reviewed in Aerts et al., 1987).

2.1.8. Force–length factor

The relationship between normalized force (F_{FL}) and muscle fibre lengths (FL) has been approximated for mammalian skeletal muscle (Woittiez et al., 1984; Epstein and Herzog, 1998) and accords to the following equation:

$$F_{FL} = -6.25\left(\frac{FL}{FL_0}\right)^2 + 12.5\left(\frac{FL}{FL_0}\right) - 5.25, \quad (13)$$

with FL_0 the optimal fibre length. To include this force–length relationship in our model, we made the following assumption: the optimal fibre length for jaw muscles from a given species is reached when the muscles are stretched according to a mouth opening of mean maximum gape angle decreased with 10°. In this situation, the jaw muscles are well adapted to work within the range of fibre lengths with favourable sarcomere-overlap and, unlikely to reach the unstable, descending limb of the force–length curve ($F_{FL} > 1.1$).

2.1.9. Muscle activation rise time

Maximal activation of muscle is not reached instantaneously, but is gradually built up. The shortest time to peak twitch force from in vitro studies on contractile properties of fast fibred fish muscles was used (20 ms; James et al., 1998). To reach maximal activation after 20 ms, a sinusoidally rising activation profile was used:

$$F_{Act} = 0.5 - 0.5\cos(\pi t/T_r), \quad (14)$$

with F_{Act} the muscle activation factor, T_R the activation rise time (20 ms) and t the time (between 0 and 20 ms). After 20 ms, full stimulation of the muscles was maintained ($F_{Act} = 1$). Activation of left and right muscles is assumed to be identical.

2.1.10. Parallel elastic force

A parallel elastic force increasing with muscle length and proportional to maximal isometric force of the jaw muscles is included in the model (F_{Par}). In our model, F_{Par} increases linearly starting from the situation when muscles are stretched to the mean maximal gape angle (for that species) decreased with 5°. In our model, F_{Par} reaches 0.03 times F_{Max} when muscle fibres are stretched to 1.5 times the optimal fibre length. This value was determined for human jaw muscles by Koolstra and Van Eijden (1996).

2.2. Kinematic analysis

In order to test the model predictions, mouth closing movements during prey capture in the four species represented in Fig. 1 were analysed. In total 16 individuals were used in the experiments (8 *Clarias gariepinus*, 4 *Clariallabes longicauda*, 2 *Gymnallabes typus* and 2 *Channallabes apus*). The *C. gariepinus* specimens were either aquarium-raised specimens of which larval stages were initially obtained from the Laboratory for Ecology and Aquaculture (Catholic University of Leuven) or specimens obtained from aquacultural facilities (Fleuren and Nooijen BV, Someren, The Netherlands). Cranial lengths (CL) of these catfish were 28.01, 28.39, 44.4, 46.1, 47.5, 47.5, 51.7 and 56.2 mm. The *C. longicauda* individuals ($CL = 32.4$, 34.7, 35.7, 49.0) and *C. apus* individuals ($CL = 22.6$, 24.2) were caught in Northern Gabon. The *G. typus* specimens ($CL = 20.80$, 22.15) were imported from the western region of tropical Africa. Animals were kept separate in 20 L test aquaria and were trained to capture food presented inside a narrow, projecting corridor (25 cm length, 8 cm width, 15 cm water height) of the aquarium, which induced the animals to feed in a position perpendicular to the camera.

Two different prey types were used: (1) a piece of cod fillet (*Gadus morhua*) of about 3 cm^3 and (2) a North Sea shrimp (*Pandalus borealis*). Both prey types were attached to a thin, plastic coated steel wire and were suspended about 5 cm above the bottom of the corridor. The cod was pinned onto the steel wire, while the shrimp was clipped around its middle.

High-speed video recordings (250 frames s^{-1}) were made from a lateral position, using a Redlake Imaging Motionscope digital high-speed video camera (shutter 1/2500). Two floodlights (600 W) provided the necessary illumination. Only those prey capture sequences that were approximately perpendicular to the camera lens were selected and retained for further analysis. To do so, lateral recordings in which skull roof, skull bottom or origin of the maxillary barbel of the opposite side of the fish was visible, were discarded. For each individual, 10 recordings (each consisting of 5 cod and 5 shrimp captures) were analysed.

Three anatomical landmarks were digitised on the recorded images using Didge (version 2.2.0, Alistair Cullum), and the horizontal (x) and vertical (y) coordinates for each point were exported to a spreadsheet. These landmarks are the interior sides of the upper and lower jaw tips and the approximate rotation point of the lower jaw. The latter landmark was digitized after careful examination of its relative position on the head using morphological drawings from the literature and X-ray photographs. To improve the accuracy of the digitizations, each point was digitized separately throughout the entire prey capture sequence.

Table 2
Average start gape, end gape and travel distance of mouth closings

Species	Initial gape	End gape	Travel distance
Clarias gariepinus[a]	32.0±9.4	11.8±7.1	20.3±7.0
Clariallabes longicauda[b]	54.7±8.8	36.1±11.4	18.6±9.3
Gymnallabes typus[c]	55.6±10.2	35.7±11.7	19.9±7.3
Channallabes apus[c]	44.1±6.3	31.4 ±8.6	12.7±6.8

All values in degrees±standard deviation.
[a]$N = 80$.
[b]$N = 40$.
[c]$N = 20$.

After data filtering (Butterworth low pass filter, cut-off frequency between 20 and 25 Hz) and differentiation, angular displacement, velocity and acceleration profiles were obtained.

2.3. Simulations

In order to compare the speed of mouth closure in the four species with increasing degree of hypertrophy of the jaw adductor muscles, model simulations were run using the species-specific biometric data (Table 1) for a large number of jaw closures in which the lower jaw starts rotating from a given gape angle referred to as the initial gape angle, and from which it performs a specific rotation of which the magnitude is referred to as the travel distance. As the initial gape and travel distance of jaw closures in vivo are highly variable and interspecific differences are often observed (Table 2), simulations were run for several initial gape angles and travel distances. The time it takes to fulfil a specific rotation was used as a relative measure of average jaw closing velocity. In simulations used in interspecific comparisons, the species cranial length was set to 30 mm, which approximates the average cranial length of the animals used in the recording sessions. To evaluate the importance of the variables used in the model (to describe the shape of the jaw system and the dynamical properties of the jaw muscles) for jaw closing speed, a sensitivity analysis was performed. In this analysis, the effects of a 10% increase or decrease of these variables on the speed of jaw closure were reported.

3. Results

3.1. Model output: forces during jaw closure

Fig. 4 gives an overview of the model output of the forces that are involved during a specific jaw closure of *C. apus*. Initially, muscular forces are mainly used to accelerate the lower jaw (Fig. 4B). After this phase, the model predicts that forces from jaw muscle activity are largely used to overcome the increasing positive pressure in the buccal cavity and the resistance from soft tissues. In all cases, the importance of drag forces on the rotation of the half-elliptic plate is negligible (Fig. 4B)

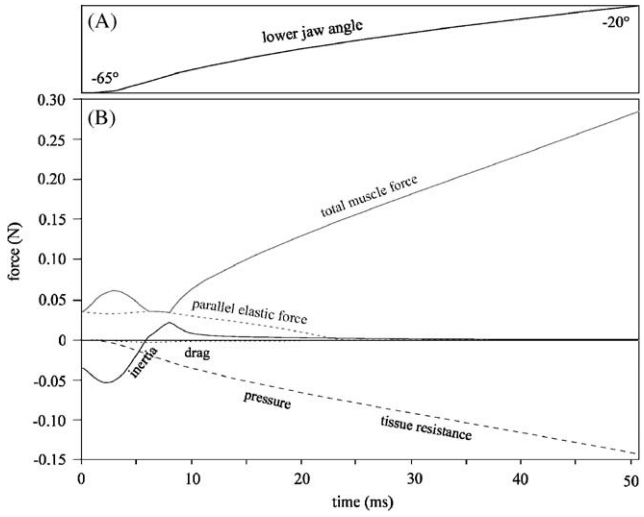

Fig. 4. Model output of the forces (graph B) involved during a simulated *C. apus* jaw closure from a lower jaw angle of −65° to −20° (graph A). The direction of the calculated forces is in between the lines of action of both muscle parts (A2A3′ and A3″). The total (active and passive) muscular force, (passive) parallel elastic forces and the forces needed to overcome drag, positive buccal pressures, tissue resistance and the inertia of the lower jaw are represented. Note that pressure and tissue resistance have equal magnitudes in the model. See text for further explanation.

As the activation of the jaw muscles is initiated at time 0, the active force production starts increasing from that moment on. Consequently, mainly the elastic forces included in the model (F_{par}) contribute to the acceleration of the lower jaw during the first millisecond of jaw closure. Once the muscles become fully active (after 20 ms), parallel elastic forces usually become an insignificant factor and in general, their overall contribution to the jaw closure is limited. However, the model predicts that these elastic forces can be much more important when clariid catfish feed at high gape angles. This is for example the case when *C. apus* opens its mouth to a −65° lower jaw angle (Fig. 4). In this case *C. apus* will have 0.035 N of parallel elastic force when it opens its lower jaw to −65°, which is about 12% of the peak total muscle force during the following jaw closure (Fig. 4B).

3.2. Model predictions vs experimental data

In general, simulations of jaw closing movements by the model correspond well to the fastest jaw closures of prey captures by the four species of clariid catfish, as determined on the high-speed video recordings (Fig. 5, first row). In all cases, the shape of the simulated kinematic profiles is realistic. For example, jaw closing

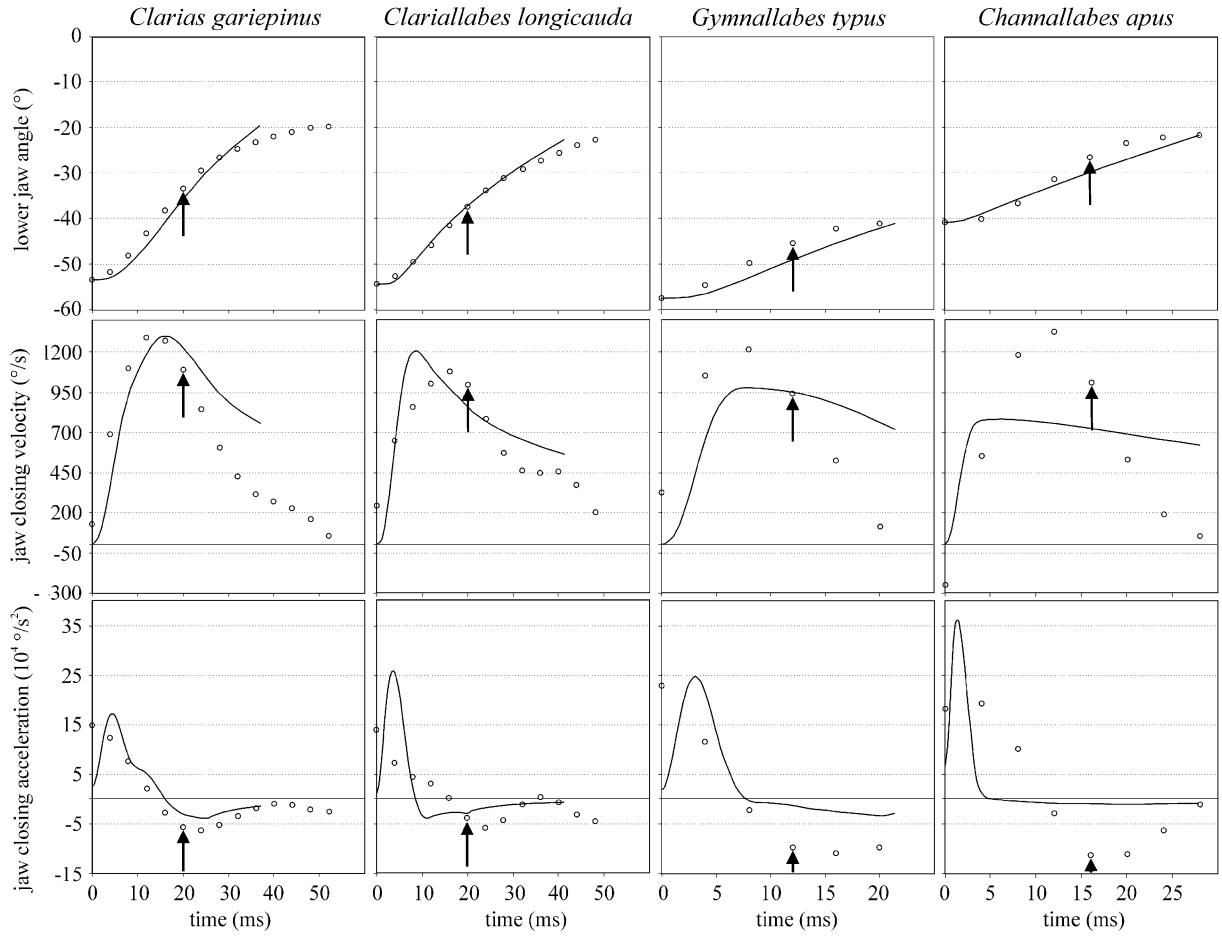

Fig. 5. Comparison of filtered kinematic profiles from the prey capture sequence in which the highest jaw closing velocity is reached for each species (dots) with the model output (black line). The model simulations are initiated and stopped at angles corresponding to initial and final gape based on the kinematic analysis. Note that the model does not account for reaction forces as a result of prey impact, and thus should not follow the kinematic data after the moment of prey impact (indicated by the arrows). Also note that the error of the kinematic data points increases from plots of angles (first row) to plots of accelerations (third row), due to data-differentiation. Consequently, a better fit between experimental data and model is expected in the graphs of lower jaw angles compared to velocities or (especially) accelerations.

velocity profiles start at zero degrees per second at the time the lower jaw is put in motion, reach their peak values in the first half of the jaw closing phase, and show a gradual decrease towards the end (Fig. 5, second row). Note, however, that effects of prey impact were not modelled. Consequently, in contrast with the model simulations, jaw closing movements based on videos of prey captures are counteracted by reaction forces from the prey after prey contact and will ultimately prevent any further movement of the lower jaw. As for the observed data, the model predicts peak accelerations to be reached within the first 5 ms of the jaw closing phase. Again, due to prey impact, the negative accelerations are much more pronounced in the kinematic data when compared to the model simulations (Fig. 5, third row).

The best match between the model and the kinematic data is for *C. gariepinus* and *C. longicuada* (Fig. 5). The time to close the mouth from its initial (maximal) opening to the moment of impacting the prey is well predicted by the model (within 10% of values from the kinematic data). Also, predictions of peak jaw closing velocities are not beyond 12% of the experimental values for these species. Peak positive accelerations, however, are apparently overestimated by the model of *C. longicauda* (Fig. 5).

In *G. typus* and *C. apus* , the kinematic data show that the peak velocities of jaw closure are underestimated by the model for these species (Fig. 5). Whereas for *G. typus*, the model prediction of peak jaw closing velocity is still not more than 20% less than the result from the kinematical analysis, a considerable difference is shown for *C. apus* (peak velocity 41% underestimated). As *C. apus* is the only species for which the velocity profiles do not accurately predict the observed in vivo results, we decided not to fine-tune the model to improve the fit for this species specifically (for example by increasing the maximal contraction velocity of the muscle fibres). Nevertheless, when comparing the model output between the four modelled species, this underestimation of maximal jaw closing velocity for *C. apus* will have to be

considered in the interpretation of the results (see Discussion).

3.3. Interspecific comparison of model output

3.3.1. Velocity of mouth closure

In most cases, no positive relation could be demonstrated between the size of the jaw muscles (Fig. 1; Table 1) and the duration of mouth closure (Fig. 6). There are, however, two exceptions: (1) jaw closures of intermediate travel distance (15°) from initial gape angles above 50° and (2) jaw closures of short travel distance (5°) from initial gape angles above 40°. Still, even in these cases, *G. typus* apparently has no advantage over *C. longicauda*, despite the fact that its jaw adductors roughly have a 50% larger physiological cross-sectional area (Table 1). Furthermore, for jaw closures of long travel distance (30°) and intermediate travel distance (15°) with initial gape angles below 45°, the species without jaw adductor hypertrophy (*C. gariepinus*) is able to carry out the fastest jaw closing movement (Fig. 6).

3.3.2. Moment and force from the jaw muscles

To illustrate the model output, the jaw closing velocity, muscular torque and force output are presented for two situations mimicking biting onto small and large prey: a jaw closure of long travel distance starting from a low gape angle (40–10°, Fig. 7) and a jaw closure of short travel distance starting from a high gape angle (55–50°, Fig. 8). As demonstrated in Fig. 6, both situations yield a different result in terms of average jaw closing velocity.

For the jaw closure with long travel distance, higher jaw closing velocities are reached during the initial phase by *C. longicauda* (during the first 4.2 ms) and *C. apus* (during the first 4.8 ms) when compared to *C. gariepinus* and *G. typus* (Fig. 7). For the latter species, the predicted jaw closing velocity is initially approximately equal to values for *C. gariepinus* but becomes significantly lower after 3.5 ms. After this initial phase, however, the species with the smallest jaw muscles (*C. gariepinus*) is able to achieve the highest mouth closing velocity (1304°/s) (Fig. 7). Peak velocities from *C. longicauda*, *G. typus* and *C. apus* are, respectively, 26.8%, 30.9% and 36.6% lower than the maximal value for *C. gariepinus*. Finally, after reaching peak values, jaw closing velocities decrease (Fig. 7). Although this drop of velocity is more substantial in *C. gariepinus* compared to the other species, the jaw closing velocity of this species remains the highest until the end of the simulated mouth closure.

The interspecific comparison of the moment of force from both jaw muscle parts (Fig. 7), shows that initially (first 2.5 ms) the magnitude of these moments is in proportion to the size of the jaw muscles: the moments increase from *C.gariepinus*, over *C. longicauda* and *G. typus* to *C. apus*. However, towards the end of the jaw closure, the moments generated by *C. gariepinus* are approximately equal to those of *C. longicauda*. Now, *G. typus* instead of *C. apus*, reaches the highest values.

Due to differences in the constructional parameters of the jaw system (length and inclination of the lower jaw in-lever, inclination of the jaw muscles; see Table 1), the interspecific comparison of jaw muscle force profiles differs from the profiles of moments (Figs. 7 and 8).

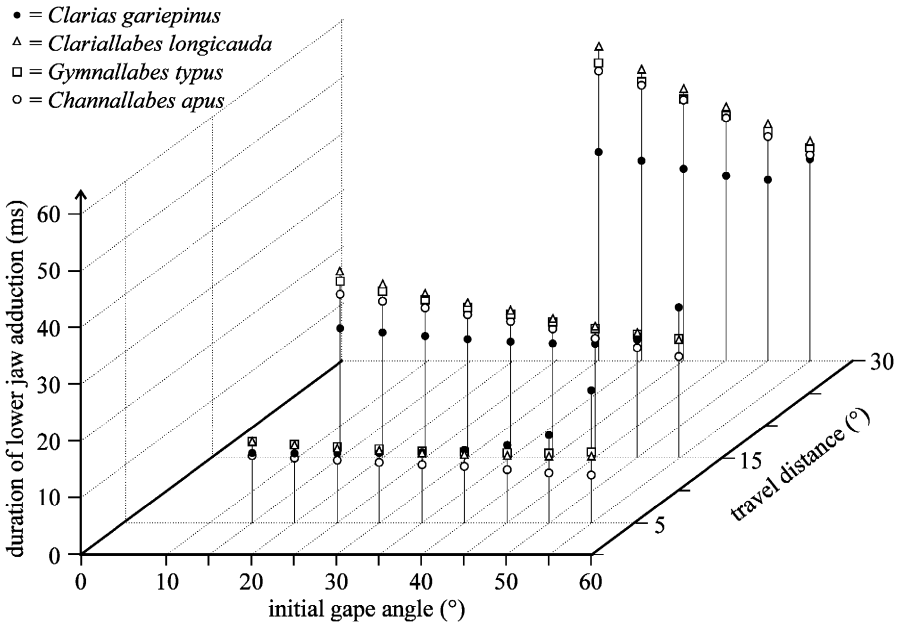

Fig. 6. Three-dimensional plot of the interspecific comparison of jaw closing time based on model simulations with different travel distances and starting from different gape angles. All species are represented by a single symbol (see legend on the upper left side). For all species, cranial length in the model was scaled to 30 mm.

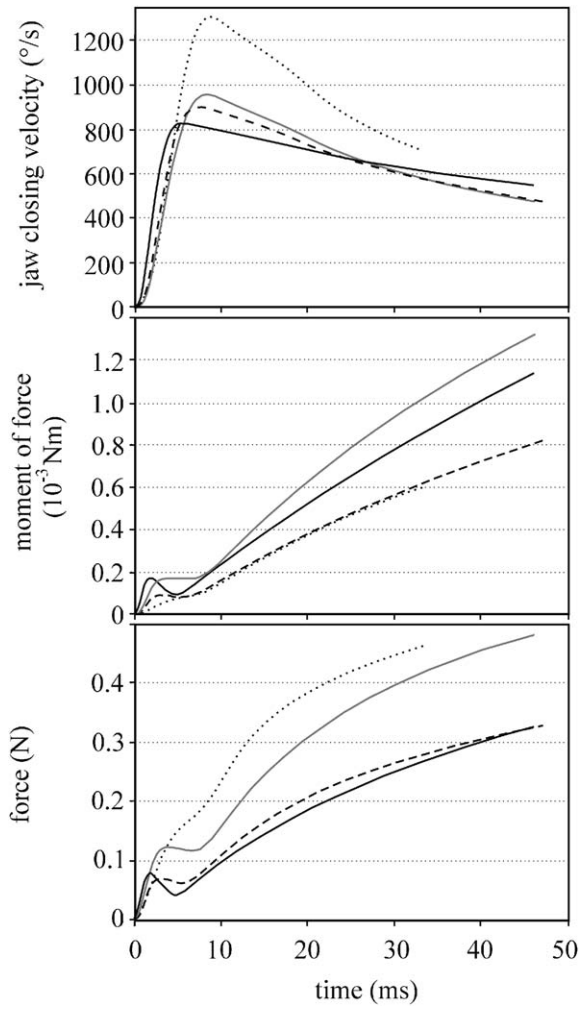

Fig. 7. Model output of a jaw closure from a gape angle of 40° to 10°. Moment of force, and force include results from both jaw closer muscles (A2A3′ and A3″). The lines represent *C. gariepinus* (dotted line), *C. longicauda* (dashed line), *G. typus* (grey line) and *C. apus* (black line).

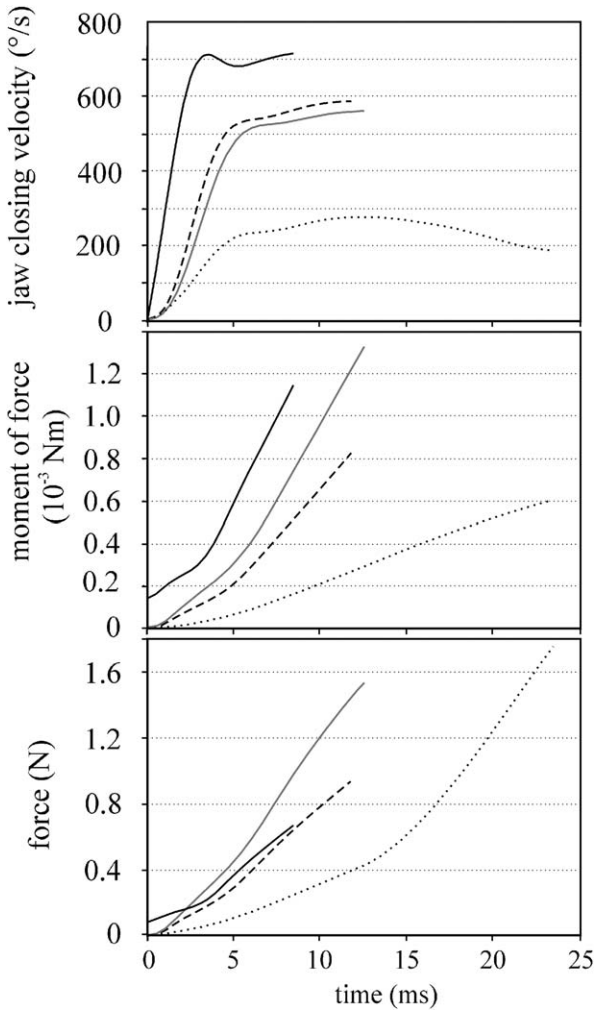

Fig. 8. Model output of a jaw closure from a gape angle of 55° to 50°. Moment of force and force include results from both muscle parts (A2A3′ and A3″). The lines represent *C. gariepinus* (dotted line), *C. longicauda* (dashed line), *G. typus* (grey line) and *C. apus* (black line).

No higher forces are generated during the 40° to 10° jaw closure in the species with enlarged jaw adductors, except for a very short interval from 0.5 to 5.5 ms after the start of the simulated jaw closure. Furthermore, after this interval, the relatively slender muscled *C. gariepinus* reaches the highest muscle forces.

In contrast with the 40° to 10° jaw rotation (Fig. 7), *C. gariepinus* shows an impaired capactity to close the mouth quickly during a short rotation that starts at a large gape angle (Fig. 8). In this case, the highest jaw closing velocity is reached by *C. apus*, followed by *C. longicauda*, *G. typus*, and *C. gariepinus*. As a result of the short travel distance (5° rotation), velocities are still rising when the end of the simulation is reached. The moment of force profiles follow the trend of increasing jaw adductor size in the species studied (Fig. 8). The same is true for the force profiles of *C. gariepinus*, *C. longicauda* and *G. typus*, while the extremely hypertrophied jaw muscles of *C. apus* generate forces that are lower than the less hypertrophied *G. typus* (Fig. 8).

3.3.3. Effects of increasing jaw muscle cross-sectional area

Previous results might suggest that hypertrophy of the jaw adductors in Clariidae (the most obvious modification of the jaw system of the species used in the present study) is of no use for generating higher jaw closing velocities, except when feeding at high gape angles and short travel distances. However, when we increase the physiological cross sectional area (PCSA) of the jaw muscles in *C. gariepinus* in the model to values equal to PCSAs from the other species, we see that the mouth can be closed significantly faster (Fig. 9A). The inverse effect is observed when the PCSA of *C. apus*, the species with most extreme jaw closer hypertrophy, is decreased

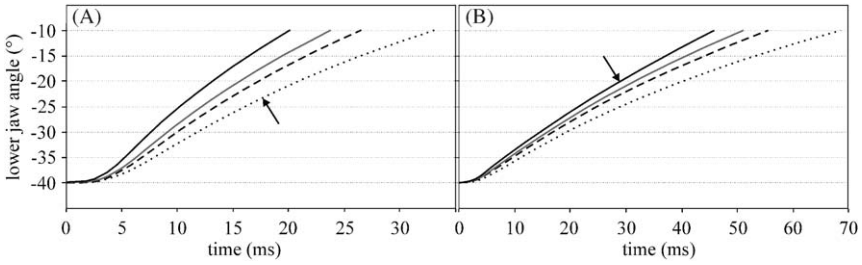

Fig. 9. (A) Jaw rotation profile of *C. gariepinus* (line indicated by arrow) together with the profiles derived from a simulation where the physiological cross-sectional area (PCSA) of the muscles is increased to values observed for the other species. In (B), the jaw rotation profile of *C. apus* (arrow) is presented together with results of simulations using a decreased value for PCSA, again corresponding to the values measured for the other species. Dotted line = PCSA of *C. gariepinus*, dashed line = PCSA of *C. longicauda*, grey line = PCSA of *G. typus* and black line = PCSA of *C. apus*.

to values equal to the species with less large jaw muscles (Fig. 9B).

The simulations with a range of PCSA values in the jaw system of *C. gariepinus* (Fig. 9A) and *C. apus* (Fig. 9B) reveal a clear difference in jaw closing velocity independent of the size of the cross-sectional area. Indeed, the *C. gariepinus* jaw system is able to fulfil the 40° to 10° jaw closure in about half the time the *C. apus* jaw system needs with an equal PCSA. Therefore, other interspecific differences in the jaw system besides PCSA are also important, and cancel out the potentially faster jaw closure due to jaw adductor enlargement for this specific jaw closing movement.

4. Discussion

4.1. The role of enlarged jaw adductors in Clariidae

Our model simulations of jaw closing movements show different results, depending on the rotation of the lower jaw that is being considered (Figs. 6 and 7 vs. Fig. 8). In most cases (e.g. all jaw closures with initial gape angles below 45° performing rotations of larger than 10°), the jaw systems of clariid species with enlarged jaw adductors is not well suited to perform fast mouth closures (Fig. 6). The observed underestimation of peak and average jaw closing velocity before prey impact of, respectively, 40% and 10% in *C. apus* (Fig. 5) will not change this result. Even if we correct for this 10% underestimation of average jaw closing velocity in *C. apus*, *C. gariepinus* is still able to perform the fastest mouth closures.

Yet, even for the lower jaw rotations in which the species with jaw adductor hypertrophy perform much poorer than the non-hypertrophied species (e.g. the 40° to 10° rotation), the size of the jaw muscles remains an important aspect for fast mouth closing in these fishes. Indeed, if *C. gariepinus* would have had jaw muscle the size of those of *C. apus*, our model suggests that it would be able to close its mouth from a 40° to 10° gape angle within 20.1 ms instead of 33.2 ms; i.e. one-third faster (Fig. 9A). The same is true for *C. apus*: a decrease in the cross-sectional area of its jaw muscles results in considerably lower speeds of jaw closure (Fig. 9B). However, when we compare the species shown in Fig. 1, the enlarged jaw muscles work within jaw systems that show other difference besides the differences in the size of the jaw muscles (Table 1). Consequently, while the jaw muscle enlargement speeds up jaw closure considerably, this effect is cancelled out if the different sized muscles are placed in their respective jaw systems.

On the other hand, an advantage in average jaw closing velocity (or in time to fulfil a certain lower jaw adduction) is predicted for short lower jaw rotations and prey captures with large gapes (Fig. 6). In addition, compared to the non-hypertrophied *C. gariepinus*, the kinematic analysis of prey captures in clariids with enlarged jaw adductors showed that these species typically also tend to feed at these larger gape angles and indeed use shorter lower jaw rotations to grab the prey (Table 2). We included a more detailed overview of model predictions of the advantage or disadvantage in jaw closing velocity of the hypertrophied species compared to the non-hypertrophied species and how the experimentally observed prey captures fit in these predictions (Fig. 11). In *C. longicauda*, *G. typus* and *C. apus*, about half of all analysed prey captures have the initial gape and travel distance for which the model predicts an advantage in average jaw closing velocity of 5% and more compared to *C. gariepinus* (Fig. 11). This indicates that, given their particular prey capture behaviour, the observed specializations in the jaw system of these species are still functionally important in vivo when it comes to fast jaw closing.

The species with enlarged jaw adductors thus appear "adapted" to feed at higher gape angles when compared to *C. gariepinus*. Biometric data also show that they have an increased inclination of the jaw muscles and a larger and more inclined lower jaw in-lever (Table 1). These characteristics of the jaw system enable the jaw muscles to continue generating torques resulting in lower jaw adduction when the lower jaw is depressed to large gape angles (Gans and De Vree, 1987). Note that

when *C. gariepinus* starts its jaw closing movement from a gape angle higher than 52.7°, the line of action of the A2A3′ jaw muscle initially lies behind the articulation of the lower jaw. Consequently, in this situation the A2A3′ muscle cannot contribute to the mouth closing movement. For the other species, the gape angle by which this occurs is considerably higher (*C. longicauda*: 67.9°, *G. typus*: 66.2° and *C. apus*: 81.8°). This suggests that the advantage for jaw closing in these species compared to *C. gariepinus* is largely due to the geometry of their jaw system, and would also occur without the hypertrophy of the jaw muscles. However, the model predicts that the range of jaw closures in which this advantage occurs would be strongly restricted if all species would have jaw muscles the size of those of *C. gariepinus* (Fig. 11). For example, whereas for jaw closures in which *C. longicauda* would have a velocity advantage of 5% compared to *C. gariepinus* with equal sized jaw muscles, an advantage of 30% is predicted with the observed hypertrophy of the jaw adductors (Fig. 11). Thus, not only when feeding at intermediate gape angles (Fig. 9), but also for feeding at high gape angles the increased size of the jaw adductors will increase jaw closing velocity considerably. However, only when feeding at large gape angles (and also for short jaw closings at lower gape angles) the species with enlarged jaw muscles are expected to have an increased jaw closing performance over the species without jaw adductor hypertrophy included in this study (Fig. 11).

The maximal size of the mouth opening is a very important aspect of feeding in fishes as it may limit the size of the prey the can be eaten (Keast and Webb, 1966; Schael et al., 1991; Gill, 1997; Huskey and Turingan, 2001; Magnhagen and Heibo, 2001). Especially for *G. typus* and *C. apus*, the adult head size is much smaller than for *C. gariepinus*, which can grow up to more than 1.5 m total body length (Cabuy et al., 1999). Consequently, being able of feeding at high gape angles and snapping the jaws relatively fast on large, moving prey may be an important aspect of the feeding success in these species with reduced head sizes and elongated bodies. Furthermore, engulfing the prey at a high gape angle may enable these catfishes to start biting or crushing the prey at a more caudal position at the jaws, in which much larger bite forces can be exerted on the prey (Herrel et al., 2002). The fact that the teeth are positioned more caudally on the oral jaws in these species (Cabuy et al., 1999; Devaere et al., 2001), confirms the importance of biting the prey closer to the jaw articulation.

4.2. Disadvantage for large lower jaw rotations in species with jaw hypertrophy

As the model predicts that an increased physiological cross-sectional area (PCSA) of the jaw muscles is an important aspect for fast mouth closure within the clariid species studied (Fig. 9), the question arises why a species like *C. apus* with its 5 times higher jaw muscle PCSA compared to *C. gariepinus* (Table 1) is not able to develop increased jaw closing velocities for most of the jaw closings simulated here (Figs. 6 and 11). The reason why the model predicts a considerably lower speed of jaw closure in most jaw rotations of long travel distance, despite the enlarged jaw adductors, has to be sought in the geometry of their jaw system (Table 1, Fig. 3).

Once the lower jaw starts its closing movement, fibres from the jaw muscles start shortening and, due to the force–velocity relationship, the force that can be generated by the jaw muscles drops. We noted an interspecific difference in the amount of force reduction as a result of changes in the force–velocity relationship. During mouth closure in *C. apus*, the force–velocity factor (F_{FV}, Eq. (8)) causes a much faster and more extensive drop in force compared a jaw closure of *C. gariepinus*. *G. typus* and *C. longicauda* are intermediate in this regard. For example, during the 40° to 10° gape angle simulation (Fig. 7), the active muscle force of *C. apus* is reduced to 2% of the maximal active isometric force in the first 6 ms of the jaw closure. For *C. longicauda* and *G. typus*, this force drops to 7% in the first 8 ms. In *C. gariepinus*, however, the decrease in active muscles force is limited and reaches the value of 17% of its maximal isometric force (after 16 ms).

The relation between fibre shortening velocity and jaw closing velocity explains these results (Fig. 10). To rotate the lower jaw by a given velocity, the muscle fibres of *C. apus* have to contract much faster compared to the same situation in *C. gariepinus*. Again, *C. longicauda* and *G. typus* are intermediate between these extremes (Fig. 10). As the force–velocity factor is directly related to the shortening velocity of the jaw muscle fibres, the reduction in active force for a given jaw closing velocity increases from *C. gariepinus* over *G. typus* and *C. longicauda* to *C. apus*. This stronger decrease in force will result in smaller fractions of the peak isometric force (F_{Max}) available to accelerate the lower jaw to higher velocities. In this way, the increased acceleration potential of the enlarged jaw muscles in the catfish studied will be lost relatively early during the jaw closing phase.

To facilitate further discussion, we introduce a ratio (fibre velocity transmission ratio or FVTR) describing the relationship between velocity of lower jaw rotation and fibre shortening velocity. This gape-dependent variable is calculated by dividing the decrease in gape angle (expressed in degrees) by the average decrease in length of the jaw muscle fibres (expressed in numbers of fibre lengths). The FVTR describes how efficient velocity from the muscles fibres is transmitted to a lower jaw rotation. If we assume that the jaw muscle fibres from different species have the same maximal

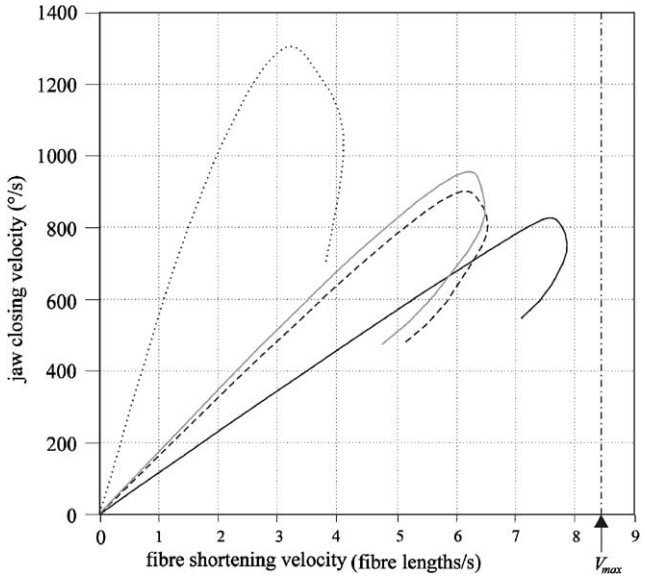

Fig. 10. Relationship between the shortening velocity of fibres from the main jaw closing muscle (adductor mandibulae A2A3′) and the angular velocity of jaw rotation during a jaw closure from 40° to 10° gape angle in *C. gariepinus* (dotted line), *C. longicauda* (dashed line), *G. typus* (grey line) and *C. apus* (black line). Note that the model input of maximal shortening velocity of the muscle fibres used in the model is 8.4 fibre length/s.

shortening velocities and if we ignore the inertial effects of the rotating lower jaw, the FVTR induces limits on the peak angular velocity that can be reached during jaw closure. Indeed, if the muscle fibres reach their maximal contraction velocity, the corresponding angular jaw closing velocity is solely determined by the FVTR. Furthermore, it describes to what extent the active jaw muscle force is decreased (due to Hill's force–velocity relationship) for a given angular jaw closing velocity.

Together with the increasing jaw adductor hypertrophy (Fig. 1), a trend can be observed in the species studied to increase (1) the length of the lower jaw in-lever, (2) the inclination of the lower jaw in-lever and (3) the inclination of the line of action of the jaw muscles (Table 1). These three changes in the geometrical constitution of the jaw system reduce the mechanical efficiency of the jaw system by decreasing the FVTR. Apparently, for lower jaw rotations of large travel distance, where higher angular jaw closing velocities are reached, the difference in FVTR among the species studied becomes increasingly important. Indeed, in Fig. 10 we see that *C. apus* nearly reaches the maximal shortening velocity of its muscle fibres in the A2A3′ during the 40° to 10° simulated jaw closure. In this situation, due to its impaired mechanical efficiency in transmitting velocity of the muscle fibres to lower jaw rotation (FVTR), *C. apus* is unable to reach the peak jaw closing velocity that was predicted by the model for *C. gariepinus*, a species with a much higher FVTR.

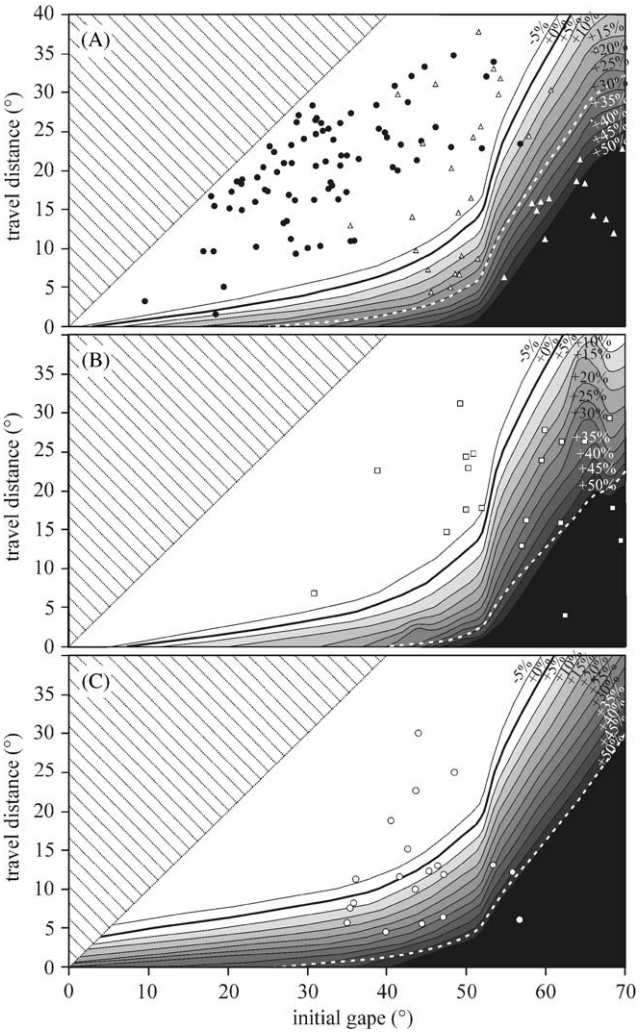

Fig. 11. Characteristics of the prey captures observed in the experiments (initial gape and travel distances of the lower jaw) plotted together with lines indicating the predicted differences in average jaw closing velocity between the species with jaw adductor hypertrophy and the non-hypertrophied *C. gariepinus*. These differences are expressed as a relative increase/decrease when comparing jaw closing times from *C. longicauda* (A), *G. typus* (B) and *C. apus* (C) to the corresponding values of *C. gariepinus* (lines connecting equal values, legends are on the upper right side of each graph). For jaw closures from the white region of a graph, the model predicts a disadvantage (+0% and lower) or very little advantage in the time needed to close the mouth (+5% and lower) for the hypertrophied clariids compared to *C. gariepinus*. In the grey or black region of the graphs, an increase of 5% and more in average jaw closing velocity is expected. Points represent the positions of all prey captures analysed based on high speed video recordings from *C. gariepinus* (black points, graph A), *C. longicauda* (white triangles, graph A), *G. typus* (white squares, graph B) and *C. apus* (white points, graph C). The white dashed line represents the +5% in average jaw closing velocity if the jaw muscles would not be hypertrophied (PCSA of *C. gariepinus* used in the model simulations of the other species).

4.3. Effects of changes in the jaw system on the speed of jaw closure

To examine what changes in the biometrics of the jaw system (see Fig. 3) are most important to improve the

performance of jaw closures in clariid catfishes, a sensitivity analysis was performed using the jaw system of the generalized clariid *C. gariepinus*. In this analysis, we changed this species jaw system characteristics from Table 1 (and also the lower jaw width) by +10% and −10% and calculated the relative change in speed of the 40° to 10° jaw closure (Fig. 12). To examine potential functional trade-offs, we also listed the effects on static bite force, kinematic efficiency of the jaw system (FVTR) and the highest possible gape angle from which the mouth can be closed (Fig. 12).

Increasing the average fibre length of the muscles is apparently the most advantageous change in the jaw system to enhance the speed of jaw closure in *C. gariepinus* for the lower jaw rotation induced here (Fig. 12). Also important are the width of the lower jaw (a narrow lower jaw reduces the moment of inertia, as well as the impact of drag and pressure on the lower jaw rotation), the length of the lower jaw in-lever (a shorter in-lever increases the kinematic efficiency) and the physiological cross-sectional area of the jaw muscles (a higher PCSA increases the acceleration of the lower jaw). Reducing the inclination of the jaw muscles and the lower jaw in-lever is less important for speeding up jaw closure. Changes in the average pennation angle and in the length of the lower jaw hardly influence the average jaw closing velocity for this lower jaw rotation (Fig. 12).

An increase in the PCSA of the jaw muscles does not compromises other functions of the lower jaw during feeding. However, it has been shown for clariid catfishes that this morphological modification can interfere with the mechanics of suction feeding (Van Wassenbergh et al., 2004). Also, spatial constraints may occur when accommodating an increased muscle volume into the cranial system and, as shown for cichlid fishes by De Visser and Barel (1996, 1998), this potentially limits the suction force that can be generated by the hyoid apparatus. In contrast, several other aspects of the jaw system in *C. gariepinus* may cause a direct mechanical trade-off between jaw closing performance and the maximal size of the mouth opening (Fig. 12): decreasing the length of the lower jaw in-lever, the width of the lower jaw, the inclination of the jaw muscles and the inclination of the lower jaw in-lever have positive effects on the speed of jaw closure, but limit the maximal size of the oral aperture and consequently the size of the prey that can be eaten. As predicted in previous studies (Barel, 1983;Wainwright and Richard, 1995; Westneat, 1994), our model also showed that the size of the in-lever of the lower jaw cause a trade-off between the maximal bite force that can be exerted by the lower jaw and the velocity of jaw movement. However, it should be kept in mind that these results strongly depend on the nature of the lower jaw rotation that is considered: the distance in which the lower jaw can freely travel before impacting the prey, and the position from which it starts its rotation are very important in this regard (Fig. 11).

Compared to the previously discussed effects of changes in the geometrical constitution of the jaw system in *C. gariepinus* (Fig. 12), altering the magnitudes of the moment of inertia, drag, tissue resistance and pressure only has relatively little influence on the speed of jaw closure. If we reduce these parameters by 10% for the 40° to 10° jaw closure in *C. gariepinus*, jaw closing will be, respectively, 0.15%, 0.03%, 1.8% and 1.8% faster. However, the contractile properties of the jaw muscle fibres are more important. For example, if the maximal shortening velocity is increased by 10%, the average speed of jaw closure will be 6.8% higher. Also the input values for *G* (the shape of the Hill-curve) describing the force–velocity relationship (2.5%), the maximal isometric force that can be generated by the jaw muscle fibres (3.5%) and the rise time of muscle

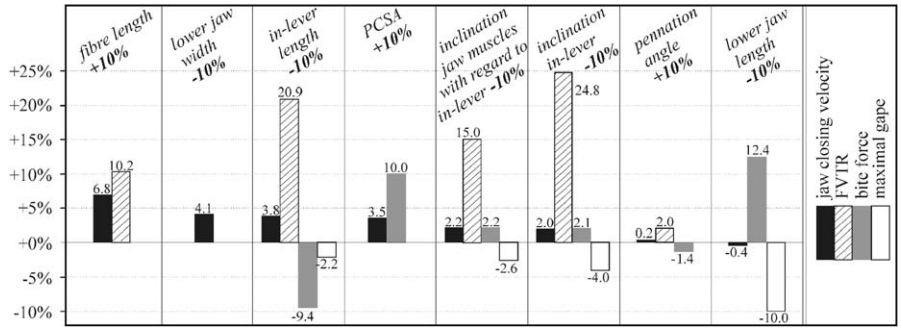

Fig. 12. Sensitivity analysis of changes in the jaw system architecture (lengths and angles +10% and −10%) of a 30 mm cranial length *C. gariepinus* performing a jaw closure of 40° to 10° gape angle. Only the changes that had an advantageous effect on the speed of jaw closure are listed, as the opposite changes (−10% instead of +10% or reversed) yielded approximately the inverse relative changes. The relative changes of the following variables are given (legends on the right side of the graphs): (1) average jaw closing velocity, (2) kinematic efficiency of the A2A3′ jaw muscle (average fibre velocity transmission ratio of 40° and 10° gape), (3) bite force perpendicular to the jaw tip (average 40° and 10° gape) and (4) the maximal gape distance from which the mouth can still be closed. In the model simulations with altered lower jaw length, the lower jaw rotation of which the absolute mouth opening corresponds to the 40° to 10° gape of normal jaw length are performed. Note that the combined effect of more than one of these changes is not always the sum of the separate effects.

activation (2.1%) appear to be important factors that affect the velocity of mouth closure. On the other hand, the parallel elastic forces (0.03%) and the optimal fibre length (0.21%) have less of an effect on the speed of jaw closure in this case. Therefore, accurate estimates of the relatively important variables are more critical for the model output than for example the values from the calculations of the moment of inertia or drag, which only seem to have a minor effect on the speed of jaw closure.

4.4. The use of jaw closing lever ratios

Previous studies dealing with the mechanics of jaw movement in teleost fishes (Richard and Wainwright, 1995; Wainwright and Richard, 1995; Wainwright and Shaw, 1999; Westneat, 1994) have used the jaw closing lever ratio (ratio of lower jaw in-lever to out-lever, or L_{in} divided by length of the lower jaw (a) in Fig. 3) as a comparative measure of potential speed of jaw closure. Also in ecomorphological studies (Albertson et al., 2003; Cutwa and Turingan, 2000; Turingan, 1994; Sibbing and Nagelkerke, 2001; Turingan et al., 1995; Wainwright and Richard, 1995; Westneat, 1995), lever ratios are used to evaluate feeding performance. When using jaw closing lever ratios as a measure of kinematical efficiency of the jaw system for closing, it is assumed that velocity of jaw movement is inversely proportional to this lever ratio. The amplification of velocity occurs in direct trade-off with the force exerted at the jaw tip, as force will be directly proportional to the lever ratio (Wainwright and Richard, 1995). Thus, in these studies, low jaw closing lever ratios are considered to enable a relatively rapid jaw closing, which is useful for capturing soft, mobile prey.

However, the results of our model show several limitations to the use of simple jaw closing lever ratios as a relative measure for speed of jaw closing in comparative studies:

(1) Kinematic efficiency of transmitting velocity from the jaw muscle fibres to the tip of the jaws includes other aspects besides length of in-lever and out-lever of the lower jaw. A sensitivity analysis on a more complete measure of kinematical efficiency (fibre velocity transmission ratio or FVTR) shows that fibre length, inclination of the jaw muscles and inclination of the in-lever are also very important parameters of the transmission system of jaw muscle to lower jaw (Fig. 12). For example, if in *C. gariepinus* the length of lower jaw in-lever is decreased by 10% (improved kinematic efficiency according to the lever theory) together with an increase in the inclination of the in-lever by 10%, the average FVTRs of the main jaw closing muscle (A2A3′) will remain equal during a rotation of 40° to 10° gape angle.

(2) Kinematic efficiency strongly depends on the gape angle: for example at a 45° gape angle, the A2A3′ muscle FVTR is 974.3°/fibre length, while at a 5° gape angle this FVTR becomes 169.2°/fibre length. Therefore, it is important to know at which gape angles the species studied usually feeds, before evaluating the kinematical efficiency of its jaw system.

(3) Our model illustrates that measures of efficiency of kinematic transmission (jaw closing lever ratios, or alternatively FVTR) cannot be simply translated to "speed of jaw closure". For the example shown in Fig. 12, the −10% change in jaw closing lever ratio only results in +3.8% average jaw closing velocity. Also relative changes in FVTR tend to overestimate the speed of jaw closure considerably in this case (Fig. 12).

(4) Our study also demonstrates that in a comparative analysis of jaw closure velocity, the result depends on the gape angle from which the jaw closure starts and on the travel distance of the jaw closure (Fig. 11). For example, if a fish feeds on very small prey and has to adduct its lower jaw over 5° only during capture, a less kinematic efficient jaw system can even be advantageous for the speed of this specific jaw closure because of its increased force transmission (increased acceleration potential).

Yet, a simple approach is often needed to evaluate the speed of jaw movement in studies that compare trophic morphologies in a broad range of species. Especially when there is no information on the orientation and the geometrical structure of the muscles attached to the lower jaw, the use of jaw lever ratios is probably the best feasible assessment of maximal jaw velocity and can provide valuable insights into the evolution of trophic structures in fishes.

Recently, a dynamical model for the analysis of jaw movements of fishes that includes muscle dynamics has been published (Westneat, 2003). Yet, in contrast to our model and dynamical models of jaw movements in humans (Koolstra, 2002; Koolstra and Van Eijden, 1996, 1997; Peck et al., 2000; Slager et al., 1997), the relationship between muscle dynamics, external load and inertial effects (established by the equation of motion) was not included. Nevertheless, these elements are rather essential to be able to predict motions from simulated muscle contractions. This could explain, for example, why the velocity profiles from the model of Westneat (2003) show jaw rotations starting with the highest velocity at time 0 after which it decreases in a hyperbolic way. Rather unexpectedly, even though this would imply infinitely high muscle forces preceding this movement, it was stated that accurate predictions of lower jaw kinematics of labrid fishes are achieved (Westneat, 2003).

4.5. Validity of our model

Like most biomechanical models, the jaw closing model of clariid catfishes presented here has its limitations, as it reduces the complexity of the real process. Inevitably, several assumptions had to be made. First, the drag forces do not include flow patterns resulting from the suction feeding event preceding, and continuing during the jaw closure phase. Secondly, muscle geometry is far more complex than included in our model. For example, we used average values for fibre length and pennation angle whereas the jaw muscles consist of fibres of different size that are placed under different angles with respect to the central tendon (Herrel et al., 2002). Thirdly, the contractile properties of the jaw muscle are taken from physiological experiments that were conducted on fish muscles other than jaw adductor muscles that were taken out of fishes from other taxonomic groups. These data could thus differ considerably from the actual contractile properties of the jaw adductor muscles of the catfishes studied in this paper. Fourthly, the magnitudes of forces resulting from pressure differences and tissue resistance in the model can be rough estimates only. However, the rather good fit between the model and the experimental data suggests that the model can be used as a tool to explore the effects of functional modifications of the jaw system in these fish, including the effects of an increased jaw muscle size on the speed of jaw closure.

Acknowledgements

Thanks to K. Leyssens and S. Nauwelaerts for discussing the topics addressed in this study. We would also like to thank L. Van Meir (Vertebrate Morphology, Ghent University) for allowing us to use her unpublished data on the morphology of *Clariallabes longicauda* and F. Ollevier and F. Volckaert for providing us with *Clarias gariepinus* larvae. W. Fleuren is acknowledged for supplying large *C. gariepinus* specimens. We are also indebted to M. Stiassny and C. Hopkins for making sampling equipment in Gabon available to us. This study was supported by the FWO Grant 6.0388.00. The authors gratefully acknowledge support of the Special Research Fund of the University of Antwerp. A.H. is a postdoctoral fellow of the fund for scientific research—Flanders (FWO-Vl).

References

Adriaens, D., Verraes, W., 1996. Ontogeny of cranial musculature in *Clarias gariepinus* (Siluroidei: Clariidae): the adductor mandibulae complex. J. Morphol. 229, 255–269.

Adriaens, D., Verraes, W., 1997. Ontogeny of the hyoid musculature in the African catfish, *Clarias gariepinus* (Burchell, 1822) (Siluroidei: Clariidae). Zool. J. Linn. Soc. 121, 105–128.

Aerts, P., Osse, J.W.M., Verraes, W., 1987. Model of jaw depression during feeding in *Astatotilapia elegans* (Teleostei: Chichlidae): mechanisms for energy storage and triggering. J. Morphol. 194, 85–109.

Aerts, P., 1990. Variability of the fast suction feeding process in *Astatotilapia elegans* (Teleostei: Cichlidae): a hypothesis of peripheral feedback control. J. Zool. London 220, 653–678.

Akster, H.A., Granzier, H.L.M., Ter Keurs, H.E.D.J., 1985. A comparison of quantitative ultrastructural and contractile characteristics of muscle fibre types of the perch *Perca fluviatilis* L. J. Comp. Physiol. 155, 685–691.

Alexander, R.McN., 1965. Structure and function in catfish. J. Zool. London 148, 88–152.

Alexander, R.McN., 2003. Principles of Animal Locomotion. Princeton University Press, Princeton.

Albertson, R.C., Streelman, J.T., Kocher, T.D., 2003. Directional selection has shaped the oral jaws of Lake Malawi cichlid fishes. Proc. Natl. Acad. Sci. USA 100, 5151–5257.

Barel, C.D.N., 1983. Towards a constructional morphology of cichlid fishes (Teleostei, Perciformes). Neth. J. Zool. 33, 357–424.

Cabuy, E., Adriaens, D., Verraes, W., Teugels, G.G., 1999. Comparative study on the cranial morphology of *Gymnallabes typus* (Siluriformes: Clariidae) and their less anguilliform relatives, *Clariallabes melas* and *Clarias gariepinus*. J. Morphol. 240, 169–194.

Cutwa, M., Turingan, R.G., 2000. Intralocality variation in feeding biomechanics and prey use in *Archosargus probatocephalus* (Teleostei, Sparidae), with implications for the ecomorphology of fishes. Environ. Biol. Fish. 59, 191–198.

Daniel, T.L., 1984. Unsteady aspects of aquatic locomotion. Amer. Zool. 24, 121–134.

Devaere, S., Adriaens, D., Verraes, W., Teugels, G.G., 2001. Cranial morphology of the anguilliform clariid *Channallabes apus* (Günther, 1873) (Teleostei: Siluriformes): are adaptations related to powerful biting? J. Zool. London 255, 235–250.

De Visser, J., Barel, C.D.N., 1996. Architectonic constraints on the hyoid's optimal starting position for suction feeding of fish. J. Morphol. 228, 1–18.

De Visser, J., Barel, C.D.N, 1998. The expansion apparatus in fish heads, a 3-D kinetic deduction. Neth. J. Zool. 48, 361–395.

Epstein, M., Herzog, W., 1998. Theoretical Models of Skeletal Muscle. Biological and Mathematical Considerations. Wiley, Chichester.

Flitney, F.W., Johnston, I.A., 1979. Mechanical properties of isolated fish red and white muscle fibres. J. Physiol. 295, 49–50.

Gans, C., De Vree, F., 1987. Functional bases of fiber length and angulation in muscle. J. Morphol. 192, 63–85.

Gibb, A.C., 1995. Kinematics of prey capture in a flatfish, *Pleuronichthys verticalis*. J. Exp. Biol. 198, 1173–1183.

Gill, A.B., 1997. The role of mouth morphology in determining threespine sickelback (*Gasterosteus aculeatus*) feeding behavior. J. Morphol. 232, 258A.

Granzier, H.L.M., Wiersma, J., Akster, H.A., Osse, J.W.M., 1983. Contractile properties of white and red fibre type of the hyohyoideus of the carp (*Cyprinus carpio* L.). J. Comp. Physiol. 149, 441–449.

Herrel, A., Adriaens, D., Verraes, W., Aerts, P., 2002. Bite performance in clariid fishes with hypertrophied jaw adductors as deduced by bite modelling. J. Morphol. 253, 196–205.

Hill, A.V., 1970. First and Last Experiments in Muscle Mechanics. Cambridge University Press, Cambridge.

Huskey, S.H., Turingan, R.G., 2001. Variation in prey-resource utilization and oral jaw gape between two populations of largemouth bass, *Micropterus salmoides*. Env. Biol. Fish. 61, 185–194.

Huysentruyt, F., Adriaens, D., Teugels, G.G., Devaere, S., Herrel, A., Verraes, W., Aerts, P., 2004. Diet composition in relation to morphology in some African aguilliform clariid catfish. Belg. J. Zool. 134, 41–46.

James, R.S., Cole, N.J., Davies, M.L.F., Johnston, I.A., 1998. Scaling of intrinsic contractile properties and myofibrillar protein composition of fast muscle in the fish *Myoxocephalus scorpius* L. J. Exp. Biol. 201, 901–912.

Johnston, I.A., 1982. Biochemistry of myosins and contractile properties of fish skeletal muscle. Mol. Physiol. 2, 15–30.

Johnston, I.A., 1983. Dynamic properties of fish muscle. In: Webb, P.W., Wheis, D. (Eds.), Fish Biomechanics. Preager, Cambridge, pp. 36–67.

Johnston, I.A., Brill, R., 1984. Thermal dependance of contractile properties of single muscle fibres from antarctic and various warm water marine fishes including the skipjack tuna (*Katsuwonus pelamis*) and kawakawa (*Euthynnus affinis*). J. Comp. Physiol. 155, 63–70.

Keast, A., Webb, D., 1966. Mouth and body form relative to feeding ecology in the fishes of a small lake, Lake Opinicon, Ontario. J. Fish. Res. Board Can. 25, 1133–1144.

Koolstra, J.H., 2002. Dynamics of the human masticatory system. Crit. Rev. Oral. Biol. Med. 13, 366–376.

Koolstra, J.H., Van Eijden, T.M.G.J., 1996. Dynamic properties of the human masticatory muscles on jaw closing movements. Eur. J. Morphol. 34, 11–18.

Koolstra, J.H., Van Eijden, T.M.G.J., 1997. Dynamics of the human masticory muscles during a jaw open-close movement. J. Biomech. 30, 883–889 doi:10.1016/S0021-9290(97)00047-X.

Lasher, W.C., 2001. Computation of two-dimensional blocked flow normal to a flat plate. J. Wind. Eng. Ind. Aerodyn. 89, 493–513 doi:10.1016/S0167-6105(00)00076-3.

Lauder, G.V., 1980. Evolution of the feeding mechanisms in primitive Actinopterygian fishes: a functional anatomical analysis of *Polypterus*, *Lepisosteus*, and *Amia*. J. Morphol. 163, 283–317.

Lauder, G.V., Norton, S.F., 1980. Assymetrical muscle activity during feeding in the Gar, *Lepisosteus oculatus*. J. Exp. Biol. 84, 17–32.

Magnhagen, C., Heibo, E., 2001. Gape size allometry in pike reflects variation betweenlakes in prey availability and relative body depth. Funct. Ecol. 15, 754–762.

Muller, M., Osse, J.W.M., 1984. Hydrodynamics of suction feeding in fish. Trans. Zool. Soc. (Lond) 37, 51–135.

Muller, M., Osse, J.W.M., Verhagen, J.H.G., 1982. A quantitative hydrodynamical model of suction feeding in fish. J. Theor. Biol. 95, 49–79.

Nagashima, T., Slager, G.E.C., Otten, E., Broekhuijsen, M.L., Van Willigen, J.D., 1997. Impact velocities of the teeth after a sudden unloading at various initial bite forces, degrees of mouth opening and distances of travel. J. Dent. Res. 76, 1751–1759.

Narici, M., 1999. Human skeletal muscle architecture studied in vivo by non-evasive imaging techniques: functional significance and applications. J. Electromyogr. Kinesiol. 9, 97–103 doi:10.1016/S1050-6411(98)00041-8.

Peck, C.C., Langenback, G.E.J., Hannam, A.G., 2000. Dynamic simulation of muscle and articular properties during human wide jaw opening. Arch. Oral. Biol. 45, 963–982 doi:10.1016/S0003-9969(00)00071-6.

Richard, B.A., Wainwright, P.C., 1995. Scaling the feeding mechanism of largemouth Bass (*Micropterus salmoides*): kinematics of prey capture. J. Exp. Biol. 198, 419–433.

Schael, D.M., Rudstam, L.G., Post, J.R., 1991. Gape limitation and prey selection in larval yellow perch (*Perca flavescens*), freshwater drum (*Aplodinotus grunniens*), and Black Crappie (*Promoxis nigromaculatus*). Can. J. Fish. Aquat. Sci. 48, 1919–1925.

Sibbing, F.A., Nagelkerke, L.A.J., 2001. Resource partioning by Lake Tana barbs predicted from fish morphometrics and prey characteristics. Rev. Fish Biol. Fisheries 10, 393–437.

Slager, G.E.C., Otten, E., Van Eijden, T.M.G.J., Van Willigen, J.D., 1997. Mathematical model of the human jaw system simulating static biting and movements after unloading. J. Neurophysiol. 78, 3222–3233.

Slager, G.E.C., Otten, E., Nagashima, T., Van Willigen, J.D., 1998. The riddle of the large loss in bite force after fast jaw-closing movements. J. Dent. Res. 77, 1684–1693.

Teugels, G.G., Adriaens, D., 2003. Taxonomy and phylogeny of Clariidae. An overview. In: Arratia, G., Kapoor, A.S., Chardon, M., Diogo, R. (Eds.), Catfishes, vol. I. Science Publishers, Enfield, pp. 465–487.

Turingan, R.G., 1994. Ecomorphological relationships among Caribbean tetraodontiform fishes. J. Zool. London. 233, 493–521.

Turingan, R.G., Wainwright, P.C., Hensley, D.A., 1995. Interpopulation variation in prey use and feeding biomechanics in Caribbean triggerfishes. Oecologia 102, 296–304.

Van Leeuwen, J.L., Muller, M., 1983. The recording and interpretation of pressures in prey-sucking fish. Neth. J. Zool. 33, 425–475.

Van Wassenbergh, S., Herrel, A., Adriaens, D., Aerts, P., 2004. Effects of jaw adductor hypertrophy on buccal expansions during feeding of air breathing catfishes (Teleostei, Clariidae). Zoomorphology 123, 81–93.

Van Willigen, J.D., Otten, E., Slager, G.E.C., Broekhuijsen, M.L., 1997. Contribution of the digastric muscles to the control of bite force in man. Arch. Oral. Biol. 42, 45–56 doi:10.1016/S0003-9969(96)00090-8.

Vogel, S., 1994. Life in Moving Fluids: The Physical Biology of Flow. Princeton University Press, Princeton.

Wainwright, P.C., Richard, B.A., 1995. Predicting patterns of prey use from morphology of fishes. Environ. Biol. Fish. 44, 97–113.

Wainwright, P.C., Shaw, S.S., 1999. Morphological basis of kinematic diversity in feeding sunfishes. J. Exp. Biol. 202, 3101–3110.

Westneat, M.W., 1994. Transmission of force and velocity in the feeding mechanism of labrid fishes (Teleostei, Perciformes). Zoomorphology 114, 103–118.

Westneat, M.W., 1995. Phylogenetic systematics and biomechanics in ecomorphology. Environ. Biol. Fish. 44, 263–283.

Westneat, M.W., 2003. A biomechanical model for analysis of muscle force, power output and lower jaw motion in fishes. J. Theor. Biol. 223, 269–281 doi:10.1016/S0022-5193(03)00058-4.

Woittiez, R.D., Huijing, P.A., Boom, H.B.K., Rozendal, R.H., 1984. A three-dimensional muscle model: a quantified relation between form and function of skeletal muscles. J. Morphol. 182, 95–113.